International Autumn School on Fundamental and Electron Crystallography (IASFEC)

PROGRAM and ABSTRACTS

October 8–13, 2017, Sofia, Bulgaria
Bulgarian Academy of Sciences

With the support of

Международната школа се организира със съдействието
на Фонд „Научни изследвания“,
договор № ДПМНФ 01/39 от 06.10.2017

International Autumn School on Fundamental and Electron Crystallography (IASFEC)

PROGRAM and ABSTRACTS

October 8–13, 2017, Sofia, Bulgaria
Bulgarian Academy of Sciences

INVITED LECTURERS

- Prof. Joke Hadermann, University of Antwerp, Belgium
- Prof. Massimo Nespolo, University of Lorraine, France
- Prof. Mois Aroyo, University of the Basque Country, Spain

ORGANIZING COMMITTEE

- Associate prof. Daniela Karashanova, PhD – Institute of Optical Materials and Technologies, BAS – chair
- Associate prof. Bogdan Ranguelov, PhD – Institute of Physical Chemistry, BAS
- Associate prof. Mihail Tarassov, PhD – Institute of Mineralogy and Crystallography, BAS
- Assoc. prof. Diana Nihtianova, PhD – Institute of Mineralogy and Crystallography, BAS
- Prof. Rosica Nicolova, PhD – Institute of Mineralogy and Crystallography, BAS
- Prof. Boris Shivachev, PhD – Institute of Mineralogy and Crystallography, BAS
- Prof. Daniela Kovacheva, PhD – Institute of General and Inorganic Chemistry, BAS
- Assoc. prof. Vladislav Kostov-Kytin, PhD – Institute of Mineralogy and Crystallography, BAS
- Assoc. prof. Zara Cherkezova – Zheleva, PhD – Institute of Catalysis, BAS
- Biliana Georgieva, PhD – Institute of Optical Materials and Technologies, BAS
- Maya Velichkova, PhD – Institute of General and Inorganic Chemistry, BAS
- Pavel Markov, PhD – Institute of General and Inorganic Chemistry, BAS
- Luben Mihaylov, PhD – Faculty of Chemistry and Pharmacy, Sofia University

SCIENTIFIC PROGRAM

Day 1: 08 October 2017, Sunday	
morning	Arrival, registration and accommodation
	Lecturer: prof. MoisAroyo
13:30 – 18:00	• Basic matrix algebra (matrix multiplication, calculation of determinant and trace)
Day 2: 09 October 2017, Monday	
8:45 – 9:00	Opening of the School (Dr. Daniela Karashanova)
	Lecturers: prof. MoisAroyo, prof. Massimo Nespolo
9:00 – 11:00	• Introduction to group theory: the notion of symmetry and symmetry groups. • Lattices and unit cells. Crystallographic symmetry in two dimensions
11:00 – 11:30	Coffee break
11:30 – 13:30	• Crystallographic symmetry in three dimensions: Bravais lattices, point groups, holohedries and merohedries, point groups; Hermann-Mauguin symbols for point groups.
13:30 – 15:00	Lunch
15:00 – 16:30	• Lattice planes, Miller indices and Bravais-Miller indices. Forms, zones and zone axes. • Choice of the zones to look at in ED for the different crystal systems. • Introduction to the stereographic projection and exercises on the stereographic projection to build crystallographic point groups.
16:30 – 17:00	Coffee break
17:00 – 18:45	• Subgroups of point groups
19:00 – 20:00	Dinner
Day 3: 10 October 2017, Tuesday	
	Lecturers: prof. MassimoNespolo, prof. MoisAroyo
9:00 – 11:00	• Metric tensor and crystallographic calculations: norm of a vector, angle between vectors, change of basis.
11:00 – 11:30	Coffee break
11:30 – 13:30	• Symmetry operations with a screw or glide component. • From point to space groups.

13:30 – 15:00	Lunch
15:00 – 16:30	• Examples and exercises on space group diagrams. • Projections of space groups and their two-dimensional symmetry.
16:30 – 17:00	Coffee break
17:00 – 18:45	• Group-subgroup relations. Klassengleiche, translationengleiche, isomorphic subgroups. Change of basis from group to subgroup. Definition and basic features of parent and daughter phases. • Integral, zonal and serial diffraction conditions. • Diffraction symbol and possible space groups corresponding to it.
19:00 – 20:00	Dinner
Day 4: 11 October 2017, Wednesday	
	Lecturers and guidance: Dr. Daniela Karashanova, Dr. Diana Nihtianova, Dr. Bogdan Ranguelov, Dr. Mihail Tarassov
09:30	Working groups at rotational principle
1/2 day	Transmission Electron Microscopy (TEM) laboratory visit
	• basics of TEM
	• sample preparation for TEM
	• experimental SAED and CBED patterns caption
1/2 day	Scanning electron microscopy (SEM) – laboratory visit
	• basics of SEM
	• sample preparation for SEM
	• Electron Back Scattered Diffraction (EBSD)
11:00 – 11:30 16:00 – 16:30	Coffee break and exchange of groups Coffee break and Poster session
13:30 – 14:45	Lunch
14:45 – 15:00	School's photo in front of the main entrance
15:00 – 17:00	Poster session
19:00 – 20:00	Dinner
Day 5: 12 October 2017, Thursday	
	Lecturer: prof. Joke Hadermann
9:30 – 11:00	• Indexing of an ED pattern. • Calculation / simulation of a SAED pattern for a given compound (from cell parameters and zone axis). • Reconstruction of the unit cell from SAED along different zone axes.
11:00 – 11:30	Coffee break

11:30 – 13:30	• Connection of the symmetry in real space to that of the ED pattern. • Analysis of the information one can obtain from CBED.
13:30 – 15:00	Lunch
15:00 – 16:30	• Differences between the symmetry information from SAED (addition of inversion centre, can't distinguish m or 2) and CBED (can distinguish all point symmetry elements). • Exercises on experimental SAED and CBED patterns
16:30 – 17:00	Coffee break
17:00 – 18:30	• From superlattices (subcells) in ED to sublattices (supercells) in real space. • Determination of point groups and space groups from ED patterns.
19:30 – 22:30	Official Dinner
Day 6: 13 October 2017, Friday	
	Lecturer: prof. Massimo Nespolo
9:30 – 11:00	• Domains (twins, antiphase domains); effect of twinning on the diffraction pattern. • Calculation of twin index, obliquity, unit cell of the twin lattice. • Splitting of reflections following a phase transition to a lower lattice system.
11:00 – 11:30	Coffee break
	Lecturer: prof. Joke Hadermann
11:30 – 13:30	• Effect of the presence of symmetry operations with a glide component on ED patterns, effect of screw axes, Gjonnes-Moodie lines • Determination of space groups from ED patterns
13:30 – 15:00	Lunch
15:00 – 16:30	• Dynamical effects of the multiple diffractions and their effect on the reflection conditions and expected equivalence of reflections. • Partial reconstruction of the space group symmetry from atomic resolution images (projection of space groups, effects of misorientation).
16:30 – 17:00	Coffee break
17:00 – 18:30	• Short introduction on the possibilities of extracting and using the reflections on ED patterns in a quantitative manner to solve structures ab initio and to refine structures. • Exercises on the determination of space group from electron diffraction patterns.
18:30 – 18:45	Concluding remarks (Dr. Daniela Karashanova)
19:00 – 21:00	Farewell dinner

Necessary background (assumed achieved by all participants):

- Interaction of radiation with matter.
- Elementary physics of scattering and diffraction. Fourier transform, atomic scattering factor and structure factor.
- Reciprocal lattice.
- Bragg‘s law and Ewald‘s sphere.

CONTENTS

X-Ray diffraction, high temperature Mössbauer and Raman spectroscopy studies of $Sr_{3-x}Ca_xFe_2TeO_9$ ($0 \leq x \leq 1$) double perovskite

Abdelhadi El Hachmi[1,*], B. Manoun[1], Y. Tamraoui[1] and P. Lazor[2]

[1] *Laboratoire des Sciences des Matériaux, des Milieux et de la modélisation (LS3M), FP Khouribga, Hay Ezzaitoune BP 145, Khouribga 25000, Université Hassan 1er, Morocco*
[2] *Department of Earth Sciences, Uppsala University, SE-752 36, Uppsala, Sweden*

*elhachmi.abdelhadi@gmail.com

Keywords: Double perovskite, $Sr_{3-x}Ca_xFe_2TeO_9$, X-ray diffraction, Raman spectroscopy.

Double perovskites with general stoichiometry $A_2BB'O_6$ (A = alkaline earths; B, B′ = transition metals) have been the topic of a large number of studies in the last few years, since the discovery of colossal magnetoresistance in Sr_2FeMoO_6 [1] and Sr_2FeReO_6 [2] because this effect is of technological interest for the detection of magnetic fields and in magnetic memory devices [3]. These materials are half-metallic ferromagnets with TC's significantly above room temperature.

X-ray diffraction and Raman spectroscopy studies of Ca substituted double perovskite compound $Sr_{3-x}Ca_xFe_2TeO_9$ with ($0 \leq x \leq 1$) were investigated. Both Rietveld refinements and Raman studies at room temperature showed that series have a tetragonal symmetry with s.g. *I*4/*m*. Phase transitions are observed by Raman spectroscopy from tetragonal to cubic structures as a function of temperature. For this series, the transitions show considerable changes in the temperature dependence of the modes: All the Raman modes show a linear behavior when temperature is increased, then the slope change dramatically indicating the symmetry change between the two systems encountered in the series. Mössbauer studies reveal the presence of iron in the 3+ oxidation state. A paramagnetic to ferromagnetic transition is observed when strontium is substituted by calcium (for $x = 0$ and $x = 0.5$ the materials are paramagnetic and when $x = 1$, the composition became magnetic).

References

[1] Kobayashi, K.-I.et al. (1998) Nature 395, 677.
[2] Kim, T.H. et al. (1999) Appl. Phys. Lett. 74, 1737.
[3] Ramirez, A.P. (1997) J. Phys.: Condens. Matter. 9, 8171.

Effect of Ru on the magnetic properties of $Ni_{50}Mn_{38}Sb_{12}$

Akhilesh K. Patel, K. G. Suresh*

Department of Physics, Indian Institute of Technology Bombay, Mumbai-400076, India

*suresh@phy.iitb.ac.in

Abstract. We report on the structural, magnetic and transport properties of Ru doped $Ni_{50}Mn_{38}Sb_{12}$ Heusler alloy. The changes in the critical temperatures with the magnetic field are examined. Apart from second order magnetic phase transition at 326 K, a first order structural transition from cubic austenite to orthorhombic martensite occurs at 265 K. Magnetocaloric effect is calculated and the magnetic entropy change in 70 kOe is found to be 12.3 $Jkg^{-1}K^{-1}$.

1. Introduction

The multi-functionality of Heusler alloys like magnetocaloric effect (MCE), shape memory effect, exchange bias, magnetoresistance, has paramount significance in condensed matter physics. In particular, MCE in these alloys is promising [1]. In recent years, numerous magnetic materials have been investigated in search of potential magnetic refrigerant materials [2]. Though, the first order magnetic phase transition materials are associated with latent heat and thermal hysteresis , these materials are found to exhibit large change in magnetic entropy (ΔS_M) at the transition temperature [2]. Recently, Ni-Mn based Heusler alloys became very promising due to their first order transition near room temperature, large MCE and shape memory effect [3, 4]. In Ni-Mn based compounds Ni-Mn-Sn, Ni-Mn-In and Ni-Mn-Sb are promising [5–8]. In this work, we studied the effect of Ru substitution for Ni in $Ni_{50}Mn_{38}Sb_{12}$.

2. Experimetnal Techniques

Polycrystalline $Ni_{46}Ru_4Mn_{38}Sb_{12}$ is prepared by arc melting the constituent elements of high purity. The ingot is melted several times to ensured the homogeneity. Magnetization is measured using SQUID-VSM (QD, USA). X-ray diffraction is carried out using PANalytical. Imaging and diffraction pattern were carried out by FEG-TEM.

3. Results and discussion

Fig. 1(a) shows the temperature dependent magnetization in 500 Oe collected using zero-field cooling (ZFC), field cooled cooling (FCC) and field –

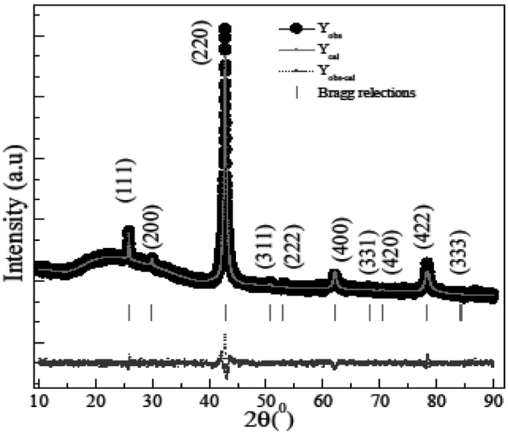

Fig. 1. Room temperature X-ray diffraction of $Ni_{46}Ru_4Mn_{38}Sb_{12}$

cooled warming (FCW) modes. The respective temperatures of martensitic, austenite and ferromagnetic phases are labeled. Magnetization isotherms at a temperature interval of 3 K around the martensitic transition temperature $T_M \sim 265$ K, are recorded (not shown here).

Using these isotherms, the magnetocaloric effect of $Ni_{46}Ru_4Mn_{38}Sb_{12}$ is estimated using the formula given below.

$$\Delta S_M(T,\Delta H) = \int_{H_0}^{H_f} \left(\frac{\partial M(T,H)}{\partial T}\right)_H dH \qquad (1)$$

Fig. 1 shows the room temperature X-ray diffraction (XRD), which crystalize in cubic with Fm–3m space group. Fig. 2 (a) shows the HRTEM image,

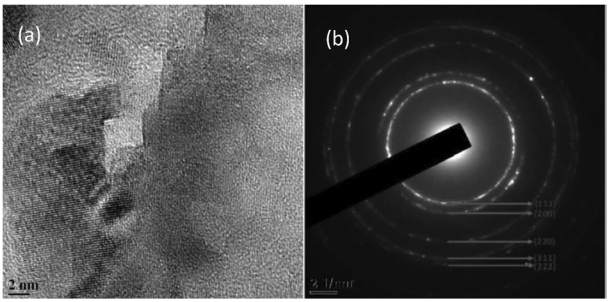

Fig. 2. (a) HRTEM image of $Ni_{46}Ru_4Mn_{38}Sb_{12}$ (b) TEM diffraction pattern of $Ni_{46}Ru_4Mn_{38}Sb_{12}$

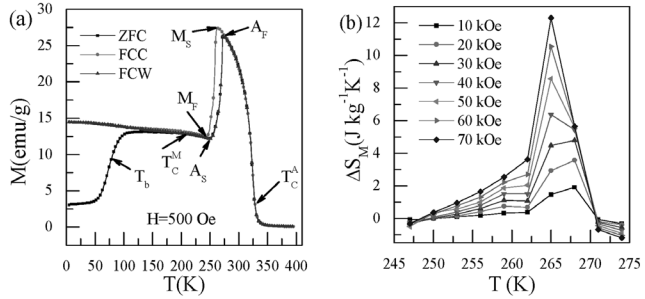

Fig. 3. (a) Temperature dependent magnetization of $Ni_{46}Ru_4Mn_{38}Sb_{12}$ in the rage of 5–400 K. The respective transition temperatures are labeled. (b) The change in magnetic entropy as a function of temperature in a few representative magnetic fields.

which shows crystalline nature. Fig. 2 (b) shows the TEM image of the sample and corresponding planes indexed by their (hkl) values, which is showed cubic structure and confirmed the X-ray diffraction

4. Conclusions

In conclusion, a detailed structural and magnetic study of Ru doped Ni-Mn-Sb based Heusler alloy is carried out using XRD, TEM and magnetization. Apart from second order magnetic phase transition at 326 K, a first order structural transition from cubic austenite to orthorhombic martensite occurs at 265 K. In particular, MCE around martensitic transition temperature is found to be about 12.3 J kg^{-1} K^{-1}.

Acknowledgement

AKP acknowledges UGC for the financial support through JRF.

References

[1] A. K. Nayak et al., 2009 J. Phys. D: Appl. Phys. **42** 035009
[2] Pecharsky et al., 1997 *Phys. Rev. Lett.* **78** 4494
[3] Ullakko K et al., 1996 *Appl. Phys. Lett.* **69** 1966
[4] Pasquale M et al., 2005 *Phys. Rev.* B **72** 094435
[5] Krenke T et al., 2005 *Nature* **4** 450
[6] Bhobe P A et al., 2007 *Appl. Phys. Lett.* **91** 242503
[7] Khan M et al., 2007 *J. Appl. Phys.* **101** 053919
[8] Du J et al., 2007 *J. Phys. D: Appl. Phys.* **40** 5523

Valorization of waste from the wood industry (sawdust) and their use as adsorbent material: physicochemical characterization, modeling and optimization adsorption using Response Surface Methodology (RSM)

Asmaa Salamat[1], Adib Merieme[1], Abdelkbir Kenz[1], Mohammed Talbi[1], M'hamed Elkouali[1], Tarik Ainane[1,2]*

[1] *Laboratory of Analytical Chemistry and Physical Chemistry of Materials, Faculty of Sciences Ben Msik, University of Hassan II, BP 7955 Casablanca 20660, Morocco*
[2] *Superior School of Technology – Khenifra (EST-Khenifra), University of Moulay Ismail, PB 170, Khenifra 54000 Morocco*

Keywords: waste, wood industry, sawdust, physicochemical characterization, modeling, optimization, RSM.

The present work reports on simple and effective ecofriendly approach for the valorization of sawdust (waste from the wood industry) in the environmental application as adsorbent biomaterials.

After determination the physicochemical properties of the tested sawdust: pH, conductivity, the biomaterial was characterized using various instrumental techniques including scanning electron microscope (SEM), energy dispersive spectroscopy (EDS) and Fourier transformed infrared spectroscopy (FTIR).

Effect of annealing temperature on the crystalline structure, growth behaviour and properties of Alnico-type thin films

Delia Patroi[1], Yuri Nikitenko[2], Vladimir Zhaketov[2], Eugen Manta[1], Eros Alexandru Patroi[1]*, Mirela Maria Codescu[1]

[1] *National Institute for R&D in Electrical Engineering INCDIE ICPE-CA, 313 Splaiul Unirii, 030138, Bucharest, Romania*
[2] *Joint Institute for Nuclear Research, Frank Laboratory of Neutron Physics, Dubna, Russia*

*eros.patroi@icpe-ca.ro, eros.patroi@gmail.com

Keywords: Alnico, Thin films, Sputtering, Rare-Earth free.

Thin films of nominal composition $Fe_{44.7}Al_{17.2}Co_{22.3}Ni_{12.7}Cu_{3.1}$ (at%) have been prepared by DC magnetron sputtering from the same composition target alloy, close to Alnico5 permanent magnets. Their structure has been studied by means of scanning electron microscopy and X-ray diffraction and reveals a partly amorphous state in the as prepared samples.

Their magnetic properties are weaker than those of a classic Alnico permanent magnet or those previously reported. The films were rapid annealed at 1000 °C, following two different ways of rapid cooling, similar to classic Alnico permanent magnets annealing procedure, then structural and magnetic properties changes were investigated. Perpendicular magnetic anisotropy was revealed while the morphology is developing from thin continuous film to a crystalline nano-particulate film.

Surface electromigration of Au on Ge(111) by Low Energy Electron Microscopy

Ali El Barraj, Stefano Curiotto, Fabien Cheynis,
Pierre Müller, Frédéric Leroy

CINaM-CNRS UMR 7325, Campus de Luminy Case 913 13288 Marseille Cedex 9, France

The project consists in studying electromigration processes [1] at surfaces in metal- semiconductor systems [2,3]. In presence of an electric current passing through a sample, an electromigration force may apply on surface atoms resulting in a global mass transfer. This force can be described as $\boldsymbol{F=Z^*eE}$, where $\boldsymbol{Z^*}$ is an effective valence, $\boldsymbol{e}$ is the electron charge and $\boldsymbol{E}$ is the applied electric field. The effective valence $\boldsymbol{Z^*}$ takes into account both the electrostatic interaction between the electric field $\boldsymbol{E}$ and the surface atom charge (charge transfer with the substrate) called the direct force and the frictional force resulting from the transfer of momentum from the charge carriers to surface atoms (wind force) [4].

We have first studied the electromigration of Au atomic layers on Ge(111) substrate. The experiments were performed *in situ* in a Ultra High Vaccum (UHV) setup equipped with a Low Energy Electron Microscope (Elmitec LEEM III microscope) [5]. The Ge(111) single crystals were cleaned in UHV and prepared by ion bombardment (Ar) and high temperature annealing (900 °C). Then approximately 0.5 ML of Au is deposited at the Ge(111) surface. Upon 640°C the Au layer forms a dilute 1×1 reconstruction whereas it rearranges into dense $\sqrt{3}\times\sqrt{3}$-R30° reconstructed domains below. We have characterized the drift motion of $\sqrt{3}\times\sqrt{3}$-domains on atomically flat terraces induced by a direct electric current ($\sim 10^6$ A.m^{-2}). The domains velocity depends on the temperature (Joules effect) and electric current. Increasing the temperature between 500–640°C, the Au domains velocity varies approximately from 30 to 800 nm.s^{-1}.

In the following figure we can see an Arrhenius plot of the Au domains velocity. The slope shows two regimes at high and low temperature. This result indicates that two main different processes of electromigration occur. However, the drift velocity is independent on the domain size showing that the elementary process of motion is dominated in both cases by a terrace diffusion process rather than periphery diffusion or attachment-detachment.

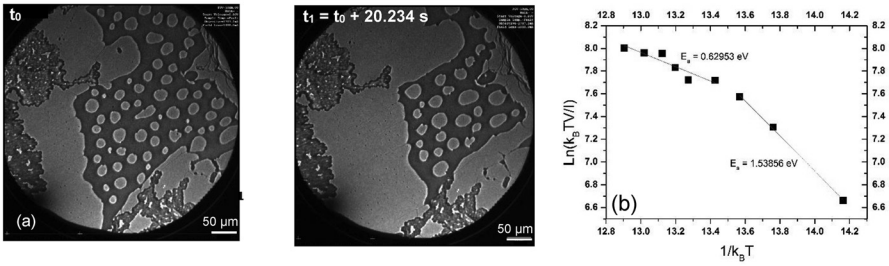

Fig. 1. (a) LEEM sequence of 2 images showing Au domains drift.
(b) Arrhenius plot of the domain velocity.

References

[1] P.S. Ho and T. kwok, Rep. Prog. Phys. 52, 301–348 (1989).
[2] H. Yasunaga and A. Natori, Surf. Sci. Rep. 15, 205–280 (1992).
[3] T. Ichinokawa et al. Phys. Rev. B 47(15) 9654 (1993).
[4] C. Tao et al., Science 328, 736–740 (2010).
[5] F. Cheynis et al. Rev. Sci. Instru. B 85 043705 (2014).

Detection and selectivity of exhaust gases tuned by hydrophobic zeolites

J. Grand[1]*, F. Dubray, S. N. Talapaneni[2] and S. Mintova[1]

[1] *Laboratoire Catalyse et Spectrochimie, Normandie Université, ENSICAEN, CNRS, 6 boulevard Maréchal Juin, 14050 Caen, France*
[2] *University of South Australia (UniSA) Mawson Lakes Campus, South Australia, SA 5095, Australia*

*julien.grand@ensicaen.fr

Nanosized MFI type zeolite nanocrystals containing different metal atoms, either incorporated in the framework (W–MFI) or extra-framework (Sn–MFI) have been prepared and assembled as homogeneous and stable films. In addition, pure-silica MFI (Si–MFI) zeolite films were prepared and used as reference samples. All zeolite nanocrystals were spin-coated on silicon wafers via a multi-step deposition using a polymer binder in order to increase the mechanical stability of the films. The obtained zeolite films were exposed to different concentrations of CO, CO_2, NO and NO_2 gases (1–100 ppm) in the presence of water (100 ppm). The influence of the localization of the metals and the hydrophobicity on their selectivity and sorption capacity towards exhaust gases was investigated by following the sorption behavior by *operando* IR spectroscopy.

The high sensitivity of both Sn-MFI and W-MFI films towards very low concentrations of exhausted gases, especially CO_2 and NO_2, in the presence

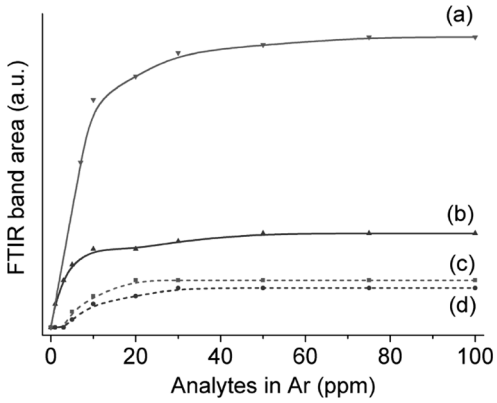

Fig. 1. Detection of CO_2 with (a) W–MFI and (c) Sn–MFI films and CO with (b) W–MFI and (d) Sn–MFI films.

of water was demonstrated (1–3 ppm). Interestingly, it has been observed that the incorporation of metal atoms in the zeolite framework, W–MFI film, leads to an increased sensibility and sorption capacity towards CO and CO_2, when compared with the extra-framework Sn–MFI film (Fig. 1). This could be explained by the higher hydrophobicity of the W-MFI material.

Acknowledgement

We acknowledge the financial support from TARGED.

References

[1] S. N. Talapaneni, J. Grand, S. Thomas, H. A. Ahmed, S. Mintova, *Materials and Design* **2016**, *99*, 574.

[2] J. Grand, S. N. Talapaneni, J.P. Gilson, S. Mintova, Patent WO2017068387A1 **2017**; J. Grand, S. N. Talapaneni, A. Vicente, C. Fernandez, E. Dib, H. A. Aleksandrov, G. N. Vayssilov, R. Retoux, P. Boullay, J.P. Gilson, V. Valtchev, S. Mintova, *Nature Mater., accepted*.

Structure of two new $K_2SnX(PO_4)_3$ (X = Cr, In) Langbeinite-type phases

H. Bellefqih*, A. Marchoud, R. Fakhreddine, N. Boudar, R. Tigha and A. Aatiq

Département de Chimie, Laboratoire de Physico-Chimie des Matériaux Appliqués, Université Hassan II de Casablanca, Faculté des Sciences Ben M'Sik, Avenue Idriss El harti, B.P. 7955, Casablanca, Morocco

*hajar.bellefqih@gmail.com

Keywords: langbeinite structure; Rietveld refinement; X-ray diffraction.

Structures of two $K_2SnX(PO_4)_3$ (X= Cr, In) phosphates, obtained by conventional solid state reaction techniques at 950 °C, were determined at room temperature from X-ray powder diffraction (XRD) using the Rietveld analysis. The two materials exhibit the Langbeinite-type structure ($P2_13$ space group, Z = 4). Cubic unit cell parameter values are: a = 9.8741(1) Å and a = 10.0460(1) Å for $K_2SnCr(PO_4)_3$ and $K_2SnIn(PO_4)_3$ respectively. Final Rietveld refinements lead to acceptable reliability factors (e.g., R_{wp} = 9.1%; R_B = 5.2% for $K_2SnCr(PO_4)_3$ and R_{wp} = 8.1%; R_B = 5.1% for $K_2SnIn(PO_4)_3$. Langbeinite frameworks are principally built of $Sn(X)O_6$ octahedra sharing corners with PO_4 tetrahedra. Structural refinements show that the two crystallographically independent octahedral sites (of symmetry 3) have a mixed Sn/X (B = Cr, In) population. The two potassium cations occupied large isolated cages within the framework.

Structural analysis of Fe/V superlattice using transmission electron microscope (TEM)

Hasan Ali

Angström Laboratory, Upsala, Sweden

hasan.ali@angstrom.uu.se

Fe/V multilayers have been used as a model system to study and explore various fundamental problems in condensed matter physics, for example thin film magnetism [1]. In such thin metallic multilayers, the physical properties of the system strongly depend on crystal quality of the structure. The crystal quality in turn is influenced by layer thickness and strain in the system. To study the effect of thickness and strain on crystal quality, Fe/V multilayers were grown with different layer thicknesses and subsequently the crystal structure and strain was determined by using different techniques.

Transmission electron microscope (TEM) was applied as a structural characterization tool to determine the layer structure and strain in one of the grown samples. The sample chosen for TEM characterization was a Fe/V superlattice (SL) with Fe = 4 and V = 28 monolayers (ML) deposited on a single crystalline MgO (001) substrate. The SL starts and ends with V layer and was capped with a palladium (Pd) layer to reduce the effects of oxidation.

The sample was prepared by using quad magnetron sputtering system. The sample stage was rotated to obtain a homogeneous deposition across the surface. The temperature of the substrate was controlled within ~1 K. The base pressure of the growth chamber was 2.7×10^{-7} Pa and was achieved using the combination of a turbo-molecular pump and a Ti sublimation pump. The targets were 99.99% pure and the Ar gas was of 99.9997% purity.

TEM sample was prepared in a cross-sectional geometry by mechanical polishing, dimple grinding and finally grazing incidence Ar ion milling. Scanning transmission electron microscope (STEM), high resolution TEM (HRTEM) and selected area diffraction (SAD) techniques were applied to determine the structure and measure the strain in the system. Fig. 1 shows a high angle annular dark field (HAAD) image of the sample. It can be seen that the layers are flat and no waviness is present. Fig. 2 shows a HRTEM image of the sample. Due to close atomic numbers of Fe and V, no clear contrast is seen between the layers. Also due to atomic steps at the MgO sub-

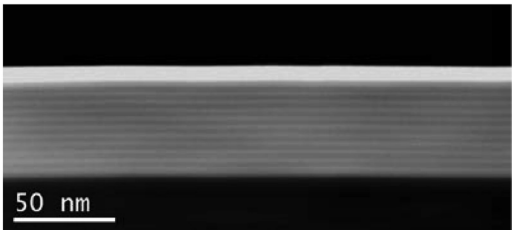

Fig. 1. HAADF image of Fe/V (4/28) SL

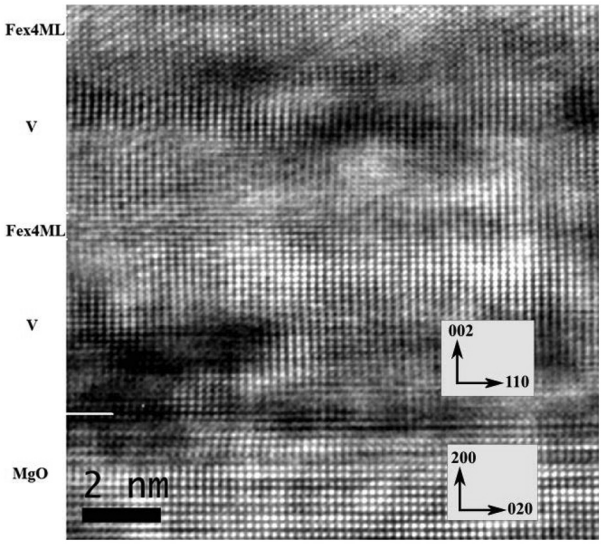

Fig. 2. HRTEM image of Fe/V (4/28) SL

strate, it is very hard to exactly mark the interfaces between Fe and V. The lattice spacings of Fe and V, both in plane and out of plane, were measured using line profiles. The strain in the system was then determined using the formula

$$\frac{d_{experimental} - d_{nominal}}{d_{nominal}} \text{ x } 100\%$$

Table. 1. Measured values of strain from Fig. 1

Element	d_{110} Nominal (Å)	d_{110} Measured (Å)	Strain %	d_{002} Nominal (Å)	d_{002} Measured (Å)	Strain %
V	2.14	2.106±0.6%	-1.4	1.515	1.58±0.8%	+4.29
Fe	2.02	2.106±0.6%	+4.45	1.43	1.32±6.5%	-7.69

The measured values of strain are given in Table. 1. These values closely match to the values measured by our collaborators using an analysis presented by Birch et al. [2].

Fig. 3 shows the SAD pattern of the sample. The SL reflections can be seen very clearly. The SL period was measured to be about 4.54 nm which agrees very well with the previously measured values by X-ray techniques.

In conclusion, we use TEM as a structural characterization tool to closely view the layering and crystal structure of Fe/V (4/28) SL deposited on MgO (001) substrate. We measure the values of lattice parameters, strain and superlattice period which closely match to the previously measured values by X-ray techniques and hence verify and strengthen those results.

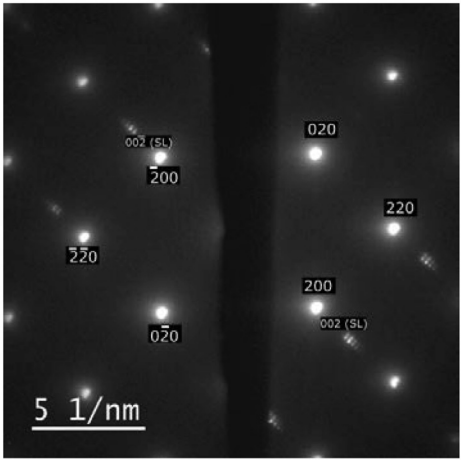

Fig. 3. SAD pattern of Fe/V (4/28) SL at the region of MgO-film interface

References

[1] B. Hjorvarsson, J. A. Dura, P. Isberg, T. Watanabe, T. J. Udovic, G. Andersson, C. F. Majkrzak, Reversible Tuning of the Magnetic Exchange Coupling in Fe/V (001) Superlattices Using Hydrogen, Phys. Rev. Lett. 79 (5) (1997) 901–904.

[2] J. Birch, J.-E. Sundgren, P. Fewster, Measurement of the lattice parameters in the individual layers of single-crystal superlattices, J Appl Phys 78 (11) (1995) 6562.

Geochemical characteristics and composition of chlorites from Elatsite PCD, Bulgaria

H. Georgieva*, R. Nedialkov

Sofia University "St. Kliment Ohridski", Faculty of Geology and Geography

*hristiana.georgieva@abv.bg

The Elatsite porphyry copper deposit (PCD), part of the Apuseni-Banat-Timok-Srednogorie copper belt, is one of the biggest and well-studied PCDs in Europe. Its ore mineralization is related to the Upper Cretaceous magmatism. A small porphyritic intrusion (Q-monzodiorite to Granodiorite) elongated in E-W direction and many porphyritic dikes are intruded in the rocks of the basement (the Vezhen Variscan granodiorite pluton and the variegated Paleozoic greenschist degree schists). Studies on the ore mineralization reveal 5 ore mineral parageneses – the hydrothermal rock alterations are determined as propylitic, high temperature K-silicate alteration, K-silicate-sericitic, Q-sericitic and quartz-adularia-carbonatic alteration.

Chlorites in Elatsite have been established through: a) propylitic alteration - with chlorite (Chl-1) replacing magmatic biotite and amphiboles; b) K-silicate-sericitic alteration-with Chl-2 replacing the hydrothermal black mica (phlogopite); c) Q-sericitic and quartz-adularia-carbonatic alterations where Chl-3 participates in the formation of nests (simultaneous) and veinlets (subsequent to the alterations).

Studying the process of chloritization is an important step for the better understanding and interpretation of the distribution of ore component of the deposit. After the electron microprobe and LA-IMS-MS analysis of chlorite from the different types of alterations is established an unequal distribution of ore elements in altered minerals. Therefore the next step in the study will be the application of electron microscopy as a method to determine the mechanism of substitution of minerals [1, 2].

References

[1] Eggleton, R. and Banfield, J.(1985) The alteration of granitic biotite to chlorite – American Mineralogist, Vol. 70, pp. 902–910.

[2] Yuguchi, T., Sasao, E., Ishibashi, M., Nishiyama, T. (2015) Hydrothermal chloritization processes from biotite in the Toki granite, Central Japan: Temporal variations of the compositions of hydrothermal fluids associated with chloritization – American Mineralogist, Vol.100, pp. 1134–1152.

Studies about M400 and M800 steel sample series using neutron diffraction measurements

Alexandru Iorga[1]*, Delia Patroi[1], Gizo Bokuchava[2], I.V. Papushkin[2], Eros-Alexandru Patroi[1], Eugen Manta[1], Florina Radulescu[1]

[1] *INCDIE ICPE-CA, Bucharest, Romania*
[2] *FLNP JINR, Dubna, Russia*

*alexandru.iorga@icpe-ca.ro

Keywords: Neutron diffraction, electrical sheets, magnetic losse.

The have been investigated structural changes in specimen series M400 and M800 by neutron TOF diffraction method. The experiments were performed on Fourier stress diffractometer FSD at the IBR-2 fast pulsed reactor in FLNP JINR (Dubna, Russia) [1, 2]. The FSD diffractometer was specially designed for residual stress studies in bulk industrial components and new advanced materials. On FSD a special purpose correlation technique is used to achieve high resolution level of the diffractometer – a combination of the fast Fourier chopper for the primary neutron beam intensity modulation and the reverse time-of-flight (RTOF) method for data acquisition [3, 4].

During the experiment on the FSD diffractometer investigated samples were installed on HUBER goniometer with flat side perpendicular to the incident neutron beam limited by diaphragm of 10×24 mm. In this way it is possible to obtain high-resolution neutron diffraction spectra $\Delta d/d \approx 2 \cdot 10^{-3}$ for backscattering detector ($2\theta = 140°$) and $\Delta d/d \approx 4 \cdot 10^{-3}$ for ±90°-detectors at $d = 2$ Å with the fairly short flight distance (~6.6 m) between Fourier chopper and neutron detectors [5].

Characterization of magnetic material was performed by measuring the magnetic properties with Single Sheet Tester – SST, for a magnetic polarization J = 50,…1500 mT, sinusoidal, at frequency f = 3,... 50 . 200 Hz according to rules DIN 50 462. The energy losses separation was performed in order to identify and reduce each component of these losses: eddy current loss (W_{cl}); hysteresis energy loss (W_h); excess loss (W_{exc}) due to eddy microcurrent that occurs at the movement of the domain walls.

References

[1] G.D. Bokuchava, V.L. Aksenov, A.M. Balagurov, V.V. Zhuravlev, E.S. Kuzmin, A.P. Bulkin, V.A. Kudryashev, V.A. Trounov, *"Neutron Fourier diffractometer FSD for internal stress analysis: first results"*, Applied Physics A: Materials Science & Processing, v.74 [Suppl1], 2002, pp s86–s88.

[2] A.M. Balagurov, G.D. Bokuchava, E.S. Kuzmin, A.V. Tamonov, V.V. Zhuk, *"Neutron RTOF diffractometer FSD for residual stress investigation"*, Zeitschrift für Kristallographie, Supplement Issue No. 23, 2006, pp. 217–222.

[3] P. Hiismäki, H. Pöyry, A. Tiitta, *"Exploitation of the Fourier chopper in neutron diffractometry at pulsed sources"*, Journal of Applied Crystallography, Vol. 21, 1988, pp. 349–354.

[4] A.M. Balagurov, I.A. Bobrikov, G.D. Bokuchava, V.V. Zhuravlev, V.G. Simkin, *"Correlation Fourier Diffractometry: 20 Years of Experience at the IBR-2 Reactor"*, Physics of Particles and Nuclei, 2015, Vol. 46, No. 3, pp. 249–276.

[5] G.D. Bokuchava, A.M. Balagurov, V.V. Sumin, I.V. Papushkin, *"Neutron Fourier diffractometer FSD for residual stress studies in materials and industrial components"*, Journal of Surface Investigation. X-ray, Synchrotron and Neutron Techniques, 2010, Vol. 4, No. 6, pp. 879–890.

Scanning electron microscopy: a direct method of identifying pollen grains

I. Piroeva*, S. Atanasova-Vladimirova

Rostislaw Kaischew Institute of Physical Chemistry, Bulgarian Academy of Sciences

*piroeva@abv.bg

A simple method of using scanning electron microscopy to observe pollen grains This method does not require freeze drying, critical point drying, or any chemical fixation procedures to prepare the specimens for scanning. Pollen grains can be identified directly from the scanning electron micrographs, thus expediting the study. The pollen has been taken from herbarium materials. It has been observed and shot with Scanning Electron Microscope (SEM) JEOL JSM-6390 without any preliminary treatment. Pollen samples has been covered by gold powder.

Shotings has been made in magnifications 900 and 15000. While the secondary electron imaging mode, the most common in use, has great value in characterizing the exine surface it is possible to obtain a more comprehensive representation of pollen grain walls by expanding the capability of the secondary mode imaging detectors.

Mesoporous nanostructured ceria-titania mixed oxide doped with copper as catalysts for sustainable environmental protection: Effect of preparation procedure

I. Genova[1]*, G. Issa[1], R. Ivanova[1], J. Henych[2], M. Dimitrov[1], D. Kovacheva[3], V. Štengl[2], T. Tsoncheva[1]

[1] *Institute of Organic Chemistry with Centre of Phytochemistry, BAS, Sofia, 1113, Bulgaria*
[2] *Materials Chemistry Department, Institute of Inorganic Chemistry AS CR*
[3] *Institute of Inorganic Chemistry, BAS, Sofia, 111, Bulgaria*

*igenova@orgchm.bas.bg

Keywords: nanostructured metal oxides, total oxidation of ethyl acetate, methanol decomposition.

Recently, the synthesis of nanostructured metal oxides has become a highly developed field and attracted the attention of the scientists in their pursuit of structural peculiarities and various unusual physical, chemical and catalytic properties. A special interest and efforts have been focused on the preparation of metal oxides with high specific surface area and/or crystalline particles in the nanosized range using various synthetic routes. It was reported that doping of titania with transition metals can increase its catalytic activity and thermal stability as a result of specific interaction and/or synergism between various metal oxide particles. The aim of current investigation is to follow the effect of copper modification procedure of mesoporous ceria-titania oxides on their catalytic behaviour in methanol decomposition to CO and hydrogen as a potential alternative fuel and ethyl acetate oxidation as a representative VOCs.

For the purpose of investigation the mesoporous ceria and/or titania oxides were synthesized by template assisted hydrothermal technique using CTAB as structure directed agent. For the first time a "chemisorption-hydrolysis" (CH) technique was applied for the copper loading on the ceria and/or titania oxides and compared with the conventional incipient wetness impregnation (WI) procedure. The copper content in all materials was about 9 wt.%. The obtained materials were studied by a complex of physicochemical techniques such as XRD, N_2 physisorption, XRD, TEM, SEM, UV-Vis, Raman and FTIR spectroscopies and TPR of H_2. The catalytic properties of the obtained materials were studied in oxidation of ethyl acetate and methanol

decomposition. High surface area mesoporous ceria-titania binary materials can be successfully synthesized using template assisted hydrothermal technique. Binary oxide supports exhibit improved dispersion, high surface area and pore volume combined with excellent oxygen mobility. Small additives of copper to ceria and/or titania oxides promoted their catalytic activity in total oxidation of ethyl acetate and methanol decomposition to syngas, but this effect is strongly influenced by preparation procedure. The applied "chemisorption-hydrolysis" technique provided formation of more homogeneously and finely dispersed copper species which also possess higher catalytic activity as compared to the conventional incipient wetness impregnation technique.

Acknowledgements

Financial support from project DM-09/4/2016 is acknowledged.

Differences in the crystallization behavior of the $Ba_{0.6}Sr_{0.4}Zn_2Si_2O_7$ phase in the presence of oxides and noble metals

L. Vladislavova[1]*, Ch. Thieme[1, 2], Ch. Rüssel[1]

[1] *Otto-Schott-Institut, Chair of Glass Chemistry I, Jena University, Fraunhoferstr. 6, 07743 Jena, Germany*
[2] *Fraunhofer Institute for Microstructure of Materials and Systems IMWS, Walter-Hülse-Str. 1, 06120 Halle, Germany*

*liliya.vladislavova@uni-jena.de

Keywords: Nucleation, Crystallization, Platinum, ZrO_2, Low thermal expansion.

The effect of different nucleation agents to the glass system BaO-SrO-ZnO-SiO_2 was studied. Glasses were melted with different concentrations of additives such as ZrO_2, TiO_2, and Pt. The obtained glass ceramics were investigated by different methods also with respect to their crystallization behavior. The crystallization kinetics of glasses from which $Ba_{1-x}Sr_xZn_2Si_2O_7$ ($0.1 \leq x \leq 0.9$) solid solution can be precipitated is of increasing interest. This phase has a similar structure to the HT phase of $BaZn_2Si_2O_7$ and possesses values of thermal expansion close to zero or even negative. Materials which do not change their dimension during heating find application e.g. in cook panels, telescope mirrors, and others.

For the characterization of the glass ceramics, X-ray diffraction was used to determine the obtained crystalline phase. The combination of light scanning microscopy and scanning electron microscopy was used to characterize the microstructure and to determine the crystallite size. Applying different heating rates in a differential scanning calorimeter, enabled to calculate the activation energy using the equations of Ozawa and Kissinger as well as the Avrami parameters, which provide further information on the crystallization process.

New insights into the effect of a wash in water on the properties of $Na_3V_2(PO_4)_2F_{3-y}O_y$ ($0 \leq y \leq 2$) materials as positive electrodes for Na-ion batteries

L. H. B. Nguyen[a,b,f], T. Broux[a,b,f], P. Sanz Camacho[a,f], T. Bamine[a,f], A. Iadecola[c,f], L. Bourgeois[d], E. Suard[e], D. Carlier[a,f], Ch. Masquelier[b,f,g] and L. Croguennec[a,f,g]

[a] *ICMCB-CNRS, Université de Bordeaux, Bordeaux INP, 87 avenue Schweitzer, 33608 Pessac Cedex (France)*
[b] *Laboratoire de Réactivité et de Chimie des Solides, CNRS-UMR#7314, Université de Picardie Jules Verne, 33 Rue Saint Leu, 80039 Amiens Cedex (France)*
[c] *Soleil Synchrotron, L'Orme des Merisiers, 91190 Saint-Aubin (France)*
[d] *ISM, Université de Bordeaux, Bordeaux INP, 33405 Talence (France)*
[e] *ILL – Institut Laue-Langevin, 38000 Grenoble (France)*
[f] *RS2E, Réseau Français sur le Stockage Electrochimique de l'Energie, FR CNRS 3459, Amiens Cedex (France)*
[g] *ALISTORE-ERI European Research Institute, FR CNRS 3104, Amiens Cedex (France)*

Sodium-ion batteries (SIBs) have recently been developed as an alternate for future sustainable energy storage system in place of the conventional lithium-ion batteries (LIBs). Amongst those which have lately been studied as positive electrode materials for SIBs, $Na_3V_2(PO_4)_2F_3$ is the most promising one due to its highly stable polyanionic framework, and its high theoretical energy density of 507 $Wh.kg^{-1}$ (128 $Ah.kg^{-1}$ at an average potential of 3.95 V *vs.* Na^+/Na) which is competitive with $LiFePO_4$ that has long been used in LIBs[1–5]. However, most of the materials reported in the literature to be $Na_3V_2(PO_4)_2F_3$ are in fact oxygen substituted ones (Fig. 1). In order

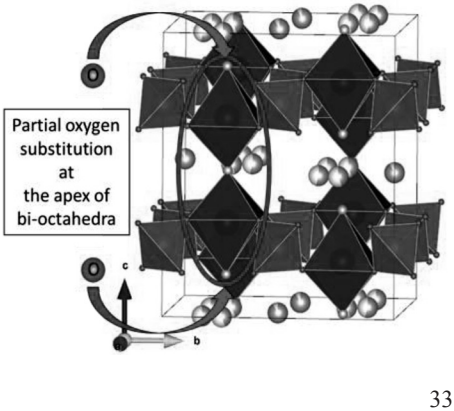

Fig. 1. 3D representation of the structure with a partial oxygen substitution for fluorine in $Na_3V_2(PO_4)_2F_{3-y}O_y$ ($0 < y \leq 2$) [6].

to determine the effect of oxygen substitution on the crystal structure and electrochemical properties of $Na_3V_2(PO_4)_2F_3$, Broux *et al.* synthesised a solid solution $Na_3V_2(PO_4)_2F_{3-y}O_y$ with y ranging between 0 and 0.5 and revealed that the richer in oxygen content, the lower the average discharge voltage is, and the sodium deintercalation mechanism evolved from a series of biphasic reactions for y = 0 to a solid solution all over the composition range up to y = 0.5 [6]. The presence of oxygen defects in these compounds can be easily detected by the use of ^{23}Na and ^{31}P MAS solid-state nuclear magnetic resonance (ss-NMR).

In this work, the study on the formation of a solid solution $Na_3V_2(PO_4)_2F_{3-y}O_y$ was extended to higher oxygen content ($0.75 \leq y \leq 2$). Furthermore, the effects of a washing in water on the crystal structure and electrochemical performance of these materials were also studied in details as: *(i)* the phases were always obtained with a small amount of impurities (Na_3VF_6 and $Na_5P_3O_{10}$) which can be easily removed by a washing in water, *(ii)* a surging interest in the electrode formulation in aqueous solution, and *(iii)* the stability of the material when stored in humid conditions has to be determined. With $y < 1$, the washing simply washed away all the undesirable impurities. When the oxygen content exceeded y = 1, the washing led to a significant change in the colour of the obtained powders and to an unexpected massive mass loss, especially for the most oxidised phase. The significant mass loss in the oxidised phases was due to the dissolution of an amorphous phase and of the crystalline decomposition products. The disappearance of the amorphous phase was clearly observed by SEM (Fig. 2).

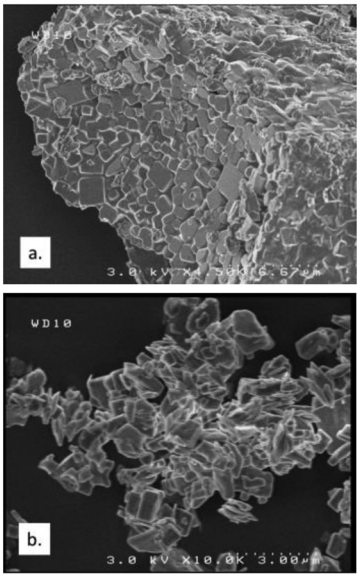

Fig. 2. SEM image of $Na_3V_2(PO_4)_2FO_2$ (y = 2) powder before washing (*a*), and after washing (*b*).

The results of our study revealed that the solid solution $Na_3V_2(PO_4)_2F_{3-y}O_y$ could be extended up to y = 1 (Fig. 3).

Despite of being reported in literature, any of our efforts to stabilise the phases with $y > 1$ always led to the formation of an amorphous phase in the presence of a crystalline one whose unit cell parameters are

similar to those of $Na_3V_2(PO_4)_2F_2O$ (y = 1), or to the decomposition of $Na_3V_2(PO_4)_2F_{3-y}O_y$ into several products, including $NaVOPO_4$, $Na_4P_2O_7$, and $NaP_{1/3}V_{2/3}O_3$.

The discovery of a solid solution formation in the composition range from y = 0 up to y = 1 was also supported by a continuous evolution in the chemical shifts on the ^{31}P MAS NMR. In $Na_3V_2(PO_4)_2F_3$, one main resonant signal was recorded at δ = 6000 ppm corresponding to the dominant presence of the $P(OV^{III})_4$ environment, the minor signal at δ = 4500 ppm was assigned to the $P(OV^{III})_3(OV^{IV})$ environment, which was created by the existence of a small amount of oxygen defect in the structure. Upon oxygen substitution, the intensity of the signal at δ = 6000 ppm diminished while new signals started to grow at δ = 3000, 1500 and 0 ppm, which are the signatures of $P(OV^{III})_2(OV^{IV})_2$, $P(OV^{III})_1(OV^{IV})_3$, and $P(OV^{IV})_4$, respectively. The intensity of the latest signal reached a maximum value with a total disappearance of other signals at y = 1.5, suggesting the sole presence of $P(OV^{IV})_4$ environment, which is in contradiction with the theoretical composition of the material (25% V^{III} and 75% V^{IV}) (Fig. 4).

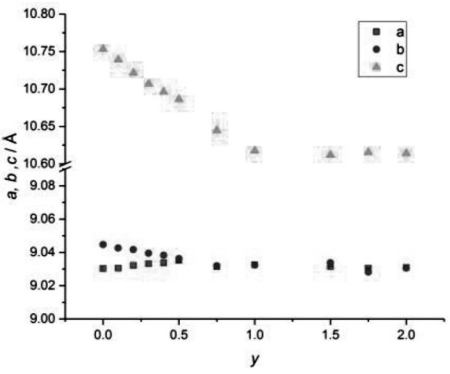

Fig. 3. The evolution of the unit cell parameters of $Na_3V_2(PO_4)_2F_{3-y}O_y$ ($0 \le y \le 2$) (Space group Amam).

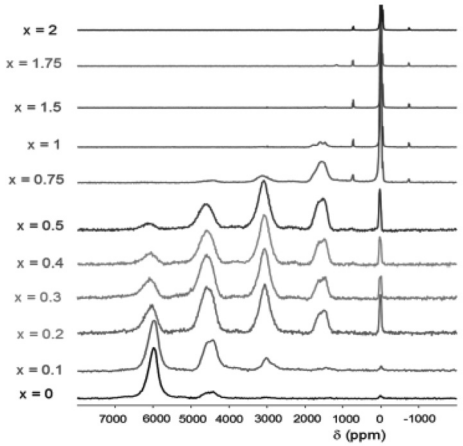

Fig. 4. ^{31}P MAS NMR spectra of $Na_3V_2(PO_4)_2F_{3-y}O_y$ ($0 \le y \le 2$) recorded with a 30 kHz spinning rate and under 2.35 T magnetic field.

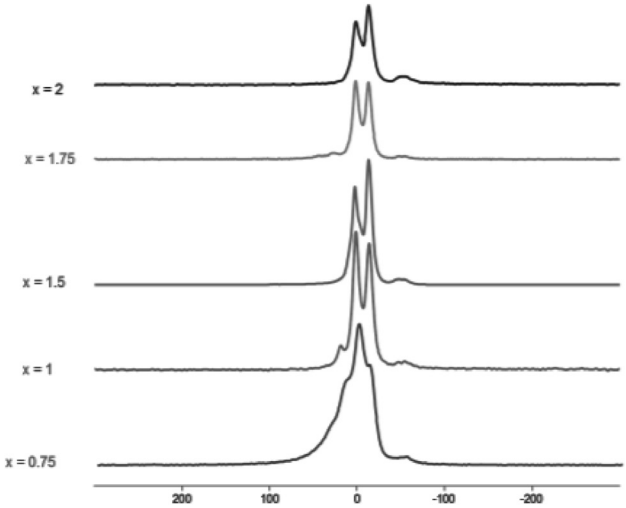

Fig. 5. A higher zoom in the diamagnetic regime of ^{31}P MAS NMR spectra of $Na_3V_2(PO_4)_2F_{3-y}O_y$ ($0.75 \leq y \leq 2$) recorded with a 30 kHz spinning rate and under 2.35 T magnetic field.

Although there was only one signal to be found on the ^{31}P MAS NMR of $Na_3V_2(PO_4)_2F_{3-y}O_y$ with y = 1.5 to 2, a higher zoom into this regime revealed the presence of a doublet with different relative intensity (Fig. 5). This finding suggested that there might be a subtle difference in the local environment in those materials.

Electrochemical tests which were performed in similar conditions for each composition of $Na_3V_2(PO_4)_2F_{3-y}O_y$ – no Carbon-coating and an applied current of C/20 – revealed that only 1.5 Na^+ ions could be extracted from the pristine material $Na_3V_2(PO_4)_2F_{3-\delta}O_\delta$ ($\delta \sim 0$) while two Na^+ ions could be de-intercalated reversibly for all the mixed valence compositions $Na_3V_2(PO_4)_2F_{3-y}O_y$ ($0 < y \leq 2$) showing an improved electronic conductivity (Fig. 6).

Acknowledgments

The authors thank SOLEIL (Gif-sur-Yvette, France) for Synchrotron X-ray spectroscopy experiments on ROCK beamline (proposal number 20160282). The authors also acknowledge the RS2E Network for the funding of LHBN's PhD thesis, as well as the financial support of Région Nouvelle Aquitaine, of

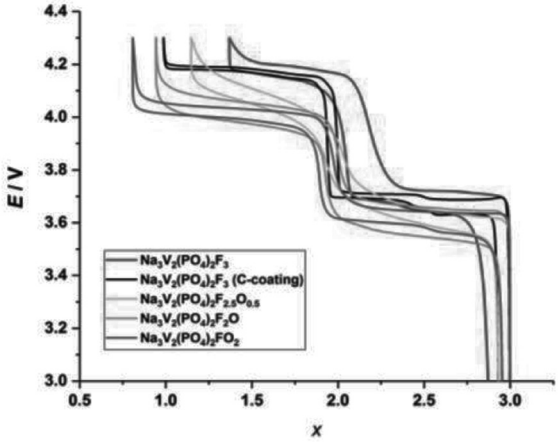

Fig. 6. The electrochemical performance of the $Na_3V_2(PO_4)_2F_{3-y}O_y$ ($0 \leq y \leq 2$) materials in sodium cells at C/20 and with the same electrode composition (Active material: C black : PVdF = 80 : 10 : 10 by wt. %).

the French National Research Agency (STORE-EX Labex Project ANR-10-LABX-76-01 and SODIUM Descartes project ANR-13- DESC-0001-02) and of the H2020 European Program (Project NAIADES).

References

[1] Le Meins *et al.*, *J. Solid State Chem.* **1999,** *148* (2), 260–277.
[2] Tsirlin *et al.*, *Phys. Rev. B* **2011**, *84*, 014429-1-16.
[3] Park *et al.*, *Adv. Funct. Mater.* **2014,** *24* (29), 4603–4614.
[4] Serras *et al.*, *Chem. Mater.* **2013,** *25* (24), 4917–4925.
[5] Bianchini *et al.*, *Chem. Mater.* **2014,** *26* (14), 4238–4247.
[6] Broux *et al.*, *Chem. Mater.* **2016**, 28, 7683–7692.

Tridymite from Alšar under the SEM-EDS and XRD investigations – evidence for silicic volcanism

M. Lazarova, T. Sijakova-Ivanova, I. Boev and B. Boev

Faculty of Natural and Technical Sciences, "Goce Delcev" University, Stip, Macedonia

Keywords: volcanism, silicic, tridymite, perlite.

This paper presents the mineralogical and geochemical investigations of tridymite and perlite using XRD, SEM-EDS methods. The volcanic caldera Alšar is located in the western area of the volcanic complex in the Kozuf Mountain at the frontier of the Vardar zone and the metamorphic complex Elen Supe, a relic of the old Precambrian continental crust. The volcanic activity in this area of the volcanic complex in the Kozuf Mountain is represented by igneous rocks with dacitic-rhyolitic composition. There are many sediment pyroclastic rocks in the composition of the caldera, represented by volcanoclastic tuffs with layers of tridymite and layers of perlite.

Tridymite appears in layers, few meters thick and its color is white. Transparent to translucent with vitreous luster. The streak is white. Hardness is 6½–7, while density is 2.28–2.33 g/cm^3. Cleavage is indistinct on {0001} and imperfect on {1010}. Tridymite and perlite are usually associated with silicic volcanism. There is also crystobalite and smaller amount of opal in tridymite's composition. The appearance of opal is due to the diagenetic changes of the high-temperature SiO_2 glass. Normalized values of the rare element earth show the distribution in the same manner as in the igneous rocks at the volcanic caldera of Alšar.

Investigation of the chemisorption of 3-aminopropylsilyl groups on silica gel using spectroscopy techniques

Miha Bukleski*

Ss. Cyril and Methodius University in Skopje, Faculty of Natural Sciences and Mathematics, Institute of Chemistry, Arhimedova 5, 1000 Skopje, Republic of Macedonia

*mihabukleski@yahoo.com

Keywords: 3-aminopropyltrimethoxysilane (APTMS), Silica gel, chemisorption, DRIFT spectra, IR studies.

The main purpose of using 3-Aminopropyltrimethoxysilane (APTMS) was to functionalize silica gel's surface for its further use in obtaining ferrocenyl derivative that can exhibit catalytic activity. APTMS has two different functional groups (amino and methoxy moieties) and can thus be used as a coupling agent (spacer), especially on silica gel as shown in Fig. 1.

The present investigation is concerned with several questions, one of which is the spectroscopic detection of chemisorbed molecules of APS on silica gel, assignment of the bands and deriving conclusions on the possible conformation and formed bonds of the chemisorbed groups. The other question concerns spectroscopic investigation of possible chemical reaction between the ferrocenyl-phosphine derivative and the APS molecules. The answer to these questions is important since it gives direct prove of a built heterogene-

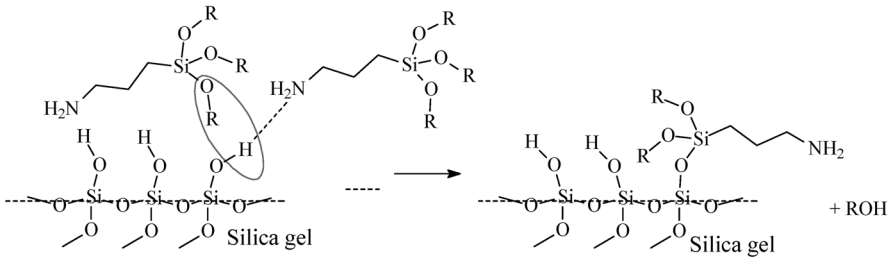

Fig. 1. Chemical reaction between the free OH groups from the activated silica gel and APTMS in anhydrous conditions

ous catalyst, because the so obtained modified silica gel with ferrocenylphosphine molecules already shows catalytic properties.

As a first step, a method for quantitative determination of the attached APTMS molecules as aminopropylsilil (APS) fragments on the silica gel's surface is proposed. The quantification was done by means of the Diffuse Reflectance Infrared Fourier Transform (DRIFT) spectroscopy technique. The appearance and vanishing of the IR bands arising from the OH, CH_2 and NH_2 vibrations were followed. The maximum amount of the APS was determined by integrating the spectra in the frequency range of the $\nu(CH_2)/\nu(CH_3)$ vibrations between 3014 and 2808 cm^{-1}. The results were further confirmed by carbon elemental analysis, AAS and BET surface measurements.

Pt(Cu) catalyst for methanol oxidation prepared by galvanic replacement on TiO_2 powder support

N. Dimitrova[1]*, J. Georgieva[1], S. Sotiropoulos[2],
Tz. Boiadjieva-Scherzer[3], E. Valova[1], S. Armyanov[1]

[1] *Rostislaw Kaischew Institute of Physical Chemistry, Bulgarian Academy of Sciences, Sofia 1113, Bulgaria*
[2] *Department of Chemistry, Aristotle University of Thessaloniki, Thessaloniki 54124, Greece*
[3] *CEST Kompetenzzentrum für elektrochemische Oberflächentechnologie GmbH, Wiener Neustadt, Austria*

*ndimitrova@ipc.bas.bg

Pt(Cu) catalyst was prepared by photodeposition of Cu on TiO_2 powder support, followed by partial galvanic replacement of Cu by Pt in a chloroplatinate solution. Pt/TiO_2 catalyst was prepared by a direct photodeposition of Pt on TiO_2 support for comparison. The surface morphology and composition of the samples were characterized by transmission electron microscopy (TEM), energy-dispersive spectrometry (EDS) and X-ray photoelectron spectroscopy (XPS). The crystal structure of the Pt(Cu)/TiO_2 and Pt/TiO_2 catalysts was examined by X-ray diffraction (XRD). The electrochemical and photoelectrochemical behavior of both platinized TiO_2 catalysts was

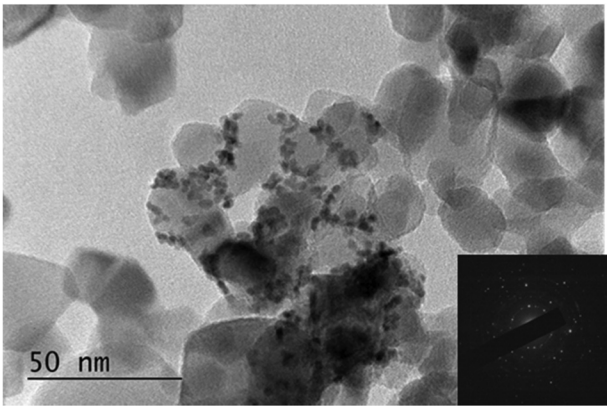

TEM micrograph and SAED image of Pt(Cu)/TiO_2 catalyst

evaluated by cyclic voltammetry, linear sweep voltammetry and chronoamperometry experiments in the dark and under UV light illumination. The electrocatalytic activity of the Pt(Cu)/TiO_2 catalyst towards methanol oxidation was evaluated and compared to Pt/TiO_2 catalyst. The Pt(Cu)/TiO_2 catalyst showed 5 times higher mass catalytic activity for methanol oxidation than a Pt/TiO_2 catalyst, further enhanced under UV light illumination. The increased catalytic activity is associated with more effective dispersion and better utilization of Pt, deposited by galvanic replacement of Cu, as well as with enhanced electron-hole separation efficiency.

Morphological characterization of organic-inorganic hybrid materials

N. Velikova[1]*, Y. Ivanova[2], I. Spassova[1]

[1] *Institute of General and Inorganic Chemistry, Bulgarian Academy of Sciences, Sofia, Bulgaria*
[2] *Department of Silicate Technologies, University of Chemical Technology and Metallurgy, Sofia, Bulgaria*

*nina.e.v@abv.bg

Keywords: Sol-gel, silsesquioxane, hybrid materials, mesoporous materials, surfactant.

The objective of this work is the synthesis of mesoporous organic-inorganic silica based materials by sol-gel method, as well as to investigate the influence of the reaction conditions on the materials morphology.

The materials were synthesized by sol-gel method by using of Pluronic P123 (nonionic triblock copolymer) as a structure directing agent, silsesquioxane (Bis[3-(trimethoxysilyl)propyl]amine ($[(CH_3O)_3Si(CH_2)_3]_2NH$)) and tetraethyl orthosilicate ($Si(OC_2H_5)_4$) under acidic condition. The materials morphology was investigated by by X-ray diffraction, Scanning Electron Microscopy, Transmission Electron Microscopy and nitrogen adsorption measurements after removing of P123 by extraction in acidic solution. Obtained samples have particle-like morphology, high values of pore size, pore volume and surface area after extraction of the used template.

Structure and magnetic properties of $Sr_3Co_2Fe_{24}O_{41}$

P. Peneva[1]*, T. Koutzarova[1], S. Kolev[1], Ch. Ghelev[1], B. Vertruyen[2], R. Closset[2], R. Cloots[2] and A. Zaleski[3]

[1] *Institute of Electronics, Bulgarian Academy of Sciences, 72 Tsarigradsko Chaussee, 1784 Sofia, Bulgaria, e-mail: petya_venelinova_peneva@abv.bg*
[2] *LSIC, Chemistry Department B6, University of Liege, Sart Tilman, B-4000 Liege, Belgium*
[3] *Institute of Low Temperature and Structure Research, PAS, 50422 Wroclaw, Poland*

*petya_venelinova_peneva@abv.bg

The multiferroics are multifunctional materials where two or more of the primary ferroic properties (*ferromagnetism, ferroelectricity, ferroelasticity, ferrotoroidicity*) coexist. The interest in magneto-electric multiferroic materials in which *ferroelectricity* and *ferromagnetism* are both present is due to the magneto-electric effect. The main requirement to the applications of the magneto-electric multiferroic materials is that the magneto-electric coupling be both large and active at room temperature and the magnetic ordering temperature be high. The Z-type hexaferrite $Sr_3Co_2Fe_{24}O_{41}$ exhibits a magneto-electric effect at room temperature.

We report studies of structural and magnetic properties of $Sr_3Co_2Fe_{24}O_{41}$ in powders and in bulk form. The precursor powders were prepared following the sol-gel auto-combustion method and synthesized at 1200 °C to produce $Sr_3Co_2Fe_{24}O_{41}$. To prepare the bulk sample, the $Sr_3Co_2Fe_{24}O_{41}$ powder was pressed, heat treated at 1200 °C for 5 hours and rapidly quenched to room temperature.

The XRD spectra of the powder showed the characteristic peaks corresponding to the Z-type hexaferrite structure as a main phase and second phases of $CoFe_2O_4$. The SEM images of the powder sample shows that the particles are well agglomerated to form clusters of different sizes and shapes. In the bulk sample, we clearly observed large regions of the hexagonal particles with a structure ordered along the *c* axis.

Magnetic phase transitions in the temperature range of 4.2–300 K were also observed connected to the different spin structure.

Microstructural characterization of black tourmaline

R. Angelov, B. Georgieva, L. Angelova and D. Karashanova*

Institute of Optical Materials and Technologies, Bulgarian Academy of Sciences, Acad. Georgy Bonchev str., bl. 109, 1113 Sofia, Bulgaria

*dkarashanova@yahoo.com

"Tourmaline" is the unifying name of a group of boron silicate minerals with common crystal structure and a large variety of elements in their composition. Together with muscovite, tourmaline is the mineral with the most

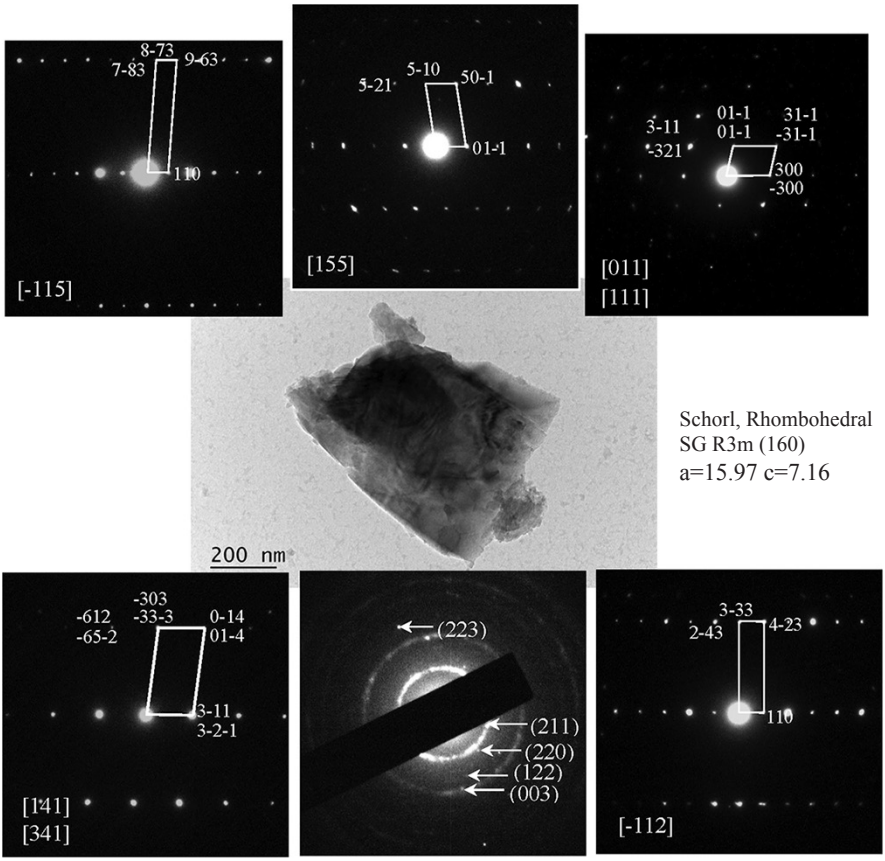

applications in the industry, due to the exceptional physical and chemical properties as high piezo and thermo-electricity, radiation in the far infrared region, significant catalytic activity etc.

The microstructure and the phase composition of black tourmaline – schorl, from Vladaya vein in Vitosha Mountain are studied by means of High Resolution Transmission Electron Microscopy (HRTEM) and XRD analysis (Phase identification according to PDF 85-1811 [PDF-2, ICDD]).

Bright field and HR TEM micrographs and selected area electron diffraction (SAED) patterns – poly- and single crystalline, received along different zone axes are presented.

Goniometry in 21-st century. Why not?

S. Dencheva

Sofia University "St. Kl. Ohridski"

stefka.dencheva@gmail.com

In the ages of nanotechnologies, modern scientists seem to have lost the taste for the classical goniometric research. But as far as I know, this is the only way to answer the question: "What simple forms actually grow in the crystal?" And this issue has not lost its relevance due to the anisotropy of the properties of substances with symmetry lower than the cubic. And if, thanks to Goldschmidt, the simple forms of "grandfathered" minerals are known, it is not so for the recently discovered and the microscopic ones.

This work aims to briefly introduce you to the author's efforts to determine the Miller's indices of simple forms of selected minerals, both at macro or micro levels.

Acknowledgements

I would like to express my acknowledgements to Prof. Georgi Kirov, who introduced me to the world of crystallography and has been supporting me in a number of studies.

Surface morphology of wine crystals

S. Atanasova-Vladimirova*, I. Piroeva

Rostislaw Kaischew Institute of Physical Chemistry, Bulgarian Academy of Sciences

*statanasova@ipc.bas.bg

Tartrates, affectionately known by industry professionals as “wine diamonds”, are tiny, crystalline deposits that occur in wines when potassium and tartaric acid, both naturally occurring products of grapes, bind together to form a crystal. It looks like sugar granules and is found at the bottom of the bottle or stuck to the stopper. In bottled wine, the presence of tartaric acid and its salts, potassium bitartrate and calcium tartrate, can result in formation of crystalline precipitates. Unpurified potassium bitartrate can take on the color of the grape juice from which it was separated.

The scanning electron microscope (SEM) views surfaces of wine crystals. They having different surface morphologies and habits were obtained: thin plates, prism faces, pyramid grain etc.

In vitro bioactive gelatin/silver containing sol-gel glasses composites: FTIR and SEM analysis

L. Radev[1]*, O. Kersten[2], I. Michailova[3], T. Dimova[4]*, Diana Zaimova[1]

[1] *University of Chemical Technology and Metallurgy, Department of Fundamental Chemical Technology, Sofia, 1756, Bulgaria*
[2] *Anhalt University of Applied Science, Department of Engineer Science, Koethen, 06366, Germany*
[3] *University of Chemical Technology and Metallurgy, Department of Silicate Technology, Sofia, 1756, Bulgaria*
[4] *Department of Pharmaceutical Science, Medical University, Varna, 9000, Bulgaria*

*biotan@abv.bg

The main objectives of the presented study is the preparation of 80BG/20G (in wt.%) composites between sol-gel glasses (BG) in the SiO_2–CaO–P_2O_5–xAg_2O (x = 0, 1, 2 and 4 wt.%) system and gelatin (G), after soaking in 1.5 SBF solutions for 12 days in static conditions. The structure and in vitro bioactivity of the prepared composites were examined by XRD and FTIR.

XRD for the composites, before soaking in 1.5 SBF solutions, revealed the presence of different $CaCO_3$ crystalline phases, such as aragonite, calcite and vaterite. In the prepared samples, XRD also detected the presence of in situ formed hydroxyapatite, accompanied with wollastonite phase. FTIR of the studied 80BG/20G composites, after soaking in 1.5 SBF solutions, proved the formation of B-type carbonate contacting hydroxyapatite (bio-apatite) on their surface. SEM-EDX results of the soaked samples show the presence of HA aggregates on the soaked surceases. On the bases of results obtained we can conclude that the synthesized BG/G composites are in vitro bioactive.

Chemical bonding and nonlinear optical properties of TeO_2–Bi_2O_3–B_2O_3 glasses

T. Tasheva*, V. Dimitrov

Department of Silicate Technology, University of Chemical Technology and Metallurgy, 8 Kl. Ohridski Blvd, 1756 Sofia, Bulgaria

*tina.tasheva@gmail.com

Oxide glasses in the system TeO_2–Bi_2O_3–B_2O_3 are prepared using a conventional melt quenching method. The polarizability approach based on the Lorentz-Lorenz equation is applied. The optical basicity and the oxide ion polarizability are estimated. The theoretical refractive index and the energy gap of the glasses are also estimated. The chemical bonding of the glasses is elucidated on the basis of the interaction parameter and the single bond strength of an average cation-oxide ion (M–O) bond.

It is found that the glasses possess relatively high values of the optical basicity and the electronic oxide ion polarizability, relatively low values for the average single bond strength and low values of the interaction parameter. The refractive index based third order nonlinear optical susceptibility of the glasses is established using generalized Miller's rule and three-photon model. The glasses possess comparatively high third order nonlinear optical susceptibility ($\sim 10^{-13}$ esu). These results indicate for the presence of weak chemical bonds which are formed between TeO_4, BiO_6, BO_4 and BO_3 groups confirmed by IR spectral analysis. Structural model of the studied glasses is proposed.

Canine seminal plasma – functions and interaction with capacitation

D. Daskalova, T. Tsvetkov*, K. Lazov, D. Gradinarska, M. Hristova, M. Ivanova

Institute of Biology and Immunology of Reproduction – BAS

*tsvetan_tsvetkov_88@abv.bg

Keywords: chromatography, seminal plasma proteins, hyperactivation, capacitation, spermatozoa.

Semen is a heterogeneous and complex cell suspension in a protein rich fluid with various functions, some of them well known, other still unexplained. The aim of the current research is focused on canine seminal plasma proteins and their functional relationship with capacitation of spermatozoa. Attempts were made to identify canine seminal plasma proteins with effect on sperm capacitation and motility. High Performance Liquid Chromatography was done and 4 seminal plasma protein fractions were obtained and further characterized by electrophoresis (7.6–200 kDa). Computer-assisted sperm analysis after incubation of spermatozoa with separated seminal plasma proteins revealed that Fraction 1, consisting of high molecular weight proteins (70–200 kDa), could increase the percentage of spermatozoa with progressive and rapid motility. Incubation with seminal plasma proteins from Fraction 1 leads to a significant increase of VCL (Curvilinear velocity) and decrease of LIN (Linearity) of spermatozoa, when compared to the other test samples and the control sample. Proteins with high molecular weight probably have the most significant influence on the process of hyperactivation and capacitation of canine spermatozoa.

Crystallochemistry of M^{2+}-hydroxysalt minerals

Z. Delcheva

Institute of Mineralogy and Crystallography – Bulgarian Academy of Sciences, "Acad. Georgi Bonchev" block 107, 1113 Sofia

zlatttt@abv.bg

The hydroxy- salt minerals form a substantial part of the mineralogical nomenclature. They are normally stable over a small range of external conditions (such as Eh, pH, T, P, concentration of solutions, component ratio, impurities, etc) as well as they are commonly associated with many other minerals of similar compositions in same parageneses. In contrast to the stable rock-forming minerals the hydroxyl-salt minerals react to slight environmental changes through changes in the crystal structure. Therefore, they are converted easily (and very often reversibly) into each other under environmental changes.

The excellent resistance of zinc and zinc-plated steel under natural conditions is due to the formation of a protective corrosion layer of zinc hydroxysalts (zinc rust). The mineral composition of this layer depends strongly on the exposure environment, and its protective effect is determined by the morphology and arrangement of the crystals [1]. The zinc hydroxy salts are also the subject of study because of some other useful properties: ion exchange and sorption properties, photocatalytic properties, hydrogen-gas sensing properties, flame retardant properties [2, 3] as well as their applicability as precursors of nanostructured ZnO for various applications [4, 5].

The mutual transformations of the Zn^{2+} hydroxyl-salt minerals with general formula $Zn^{2+}(OH)_{2-x}A_{x/n}^{n-} \cdot \pm H_2O$, where in A are SO_4^{2-} (osakaite, namuwite, lahsteinite, gordaite), Cl^- (simoncolleite), NO_3^- (synthetic NO_3-simoncolleite) and CO_3^{2-} (hydrozincite) were investigated. The bipolar character of the dominant anion (OH^-) predetermines layered character of structures of the investigated minerals [6], while the ability of Zn^{2+} ion to settle both in tetrahedral and octahedral oxygen coordination explains the specific octahedral-tetrahedral construction of the layers in Zn hydroxy-salts. The main building unit is the brucite-like layer in which one seventh (osakaite, namuwite, lahsteinite, gordaite) or one fourth (simoncolleite, hydrozincite) of the octahedral sites are vacant. The zinc cations are located on either side of the vacant octahedral positions. These ($^{tet}Zn^{2+}$) are tetrhedrally coordinated

by three OH-groups of brucite-like layers and a water molecule (in osakaite, NO_3-simoncolleite), a Cl^- anion (in gordaite and simoncolleite), O atom of CO_3^{2-} anion in hydrozincite. Thus, the octahedral-tetrahedral layer can be characterized as "interrupted decorated sheet" [7].

The interaction of minerals with chloride, nitrate, sulfate and carbonate solutions with a particular attention to the reaction mechanisms was studied. The initial and newly formed phases were mainly characterized by X-ray powder diffraction, because the powder X-ray diffraction data adequately reflect the changes in the composition of the systems. The SEM investigations were used to reveal reaction (transformation) mechanisms.

The interpretation of the mutual transformation mechanism is based on the crystal-chemical and morphological similarities between parent and new formed phase.

Two type of transformation mechanisms were found to proceed: a dissolution-precipitation process (DSP) and a solid state transformation (SST).

The results reveal the crucial role of weakly bonded components for the structure stability. Such components are non-hydroxyl anions (Cl, CO_3, SO_4, NO_3), water molecules and interlayer cations. Thus, the ratio octahedral/tetrahedral position of the layer depends on non-hydroxyl anion – sulfate anion requires formation of layer with 6:1 ratio and monodentate bonding of the anion. In the compositions with 3:1 anions dictate the formation of the structures with different symmetry: Cl^- anions cause the crystallization of the minerals with rhombohedral cell, while the CO_3^{2-}, NO_3^- – orthorhombic cell. The change of the environmental composition leads to reaction between non-hydroxyl anions of the interlayer and the solution components. As a result, new type of interlayer is formed. If it is compatible (i.e. satisfies the bond-valence requirements of the octahedral-tetrahedral layer), the solid state transformation is occurred. If during the exchange reaction, the components of the new interlayer can not form a stable system of hydrogen bonds, the crystal is destroyed and the transformation becomes trough the DSP-mechanism. In some cases, a new system of H-bonds, preserving the layer is created and transformation proceeds through SST-mechanism.

References

[1] Volovitch, P., Allely, C., Ogle, K. 2009. Understanding corrosion via corrosion product characterization: I. Case study of the role of Mg-alloying in Zn-Mg coating on steel. Corrosion science. 51, 1251–1262.

[2] Hongo, T., Lemur, T. S., Satokawa, S., Yamazaki, A. 2010. Chromate adsorption and pH buffering capacity of zinc hydroxy salts. Appl. Clay Sci. 48, 455–459.
[3] He, P., Gao, H. D., Wu, L. B., Jiang, Z. W., Wang, G. L, Li, X.M. 2013. Porous ZnO sheets transformed from zinc sulfate hydroxide hydrate and their photoluminescence performance. Acta Phys.-Chem. Shin. 29, 874–880.
[4] Moezzi, A., Cortie, M.B., McDonagh, A. M. 2013. Zinc hydroxide sulfate and its transformation to crystalline zinc oxide. Dalton Trans. 42, 14432–7.
[5] Liang, W., Li, W., Chen, H., Liu, H., Zhu, L. 2015. Exploring electrodeposited flower-like $Zn_4(OH)_6SO_4.4H_2O$ nanosheets as precursor for porous ZnO nanosheets. Electrochimica Acta. 156, 171–178.
[6] Hawthorne, F. C. 1992. The role of OH and H_2O in oxide and oxysalt minerals. Zeitschrift fur Kristallographie. 201, 183–206.
[7] Hawthorne, F. C., Schindler, M. 2000. Topological enumeration of decorated $[Cu^{2+}\phi_2]_N$ sheets in hydroxy-hydrated copper-oxysalt minerals. Can. Mineral. 38, 751–761.

Characterization of cuprite (Cu_2O) particles from waste copper cake

Gyunver Hodjaoglu

Institute of Physical Chemistry – Bulgarian Academy of Sciences (IPC-BAS)
Acad. G. Bonchev Str., block 11, 1113 Sofia, Bulgaria

e-mail: gyunver@ipc.bas.bg

Copper cake is an industrial valuable secondary waste product produced in the hydrometallurgical zinc plant after cementation stage of copper ions with zinc powder. The waste is deposited as wet sediment for export or storage. Depending on the reaction conditions the cake contains a huge amount of cuprite particles formed by cementation process and rest particles formed from the solution impurities. With the leaching and ecological aspects copper cake from KCM-Plovdiv has been treated with diluted sulphuric acid for utilization of the cuprite content. In this study the dry samples before and after leaching procedure were characterized by Scanning Electron Microscopy (SEM) for observation of the particles morphology (Cu_2O) and appearance of new reaction products ($CuSO_4$). Energy Dispersive Spectroscopy (EDS) was also applied for the chemical characterization of the observed particles. The results show that SEM-EDX is a powerful technique for initial fast determination of leaching efficiency and detection of copper sulphate micro crystals. It was found that the starting waste contains large amount of zinc sulphate whereas the final leached cake is Zn-free. The SEM analysis is very perspective for further characterizations of other types of copper-Me cakes, their chemical characterization and studying unidentified solid particles during deposition and test leaching.

Acknowledgements

The author gratefully acknowledge the financial support of Project BG05M2OP001-2.009-0023, "Establishment and development of scientific potential for the specializations of physical chemistry and electrochemistry", funded by the Operational Program "Science and Education Smart Growth", co-funded by the European Union through the European Structural and Investment Funds.

With the support of

Международната школа се организира със съдействието
на Фонд „Научни изследвания“,
договор № ДПМНФ 01/39 от 06.10.2017